Communication

The Molecular Path Approaching the Active Site in Catalytic Metal−Organic Frameworks

Ana E. Platero-Prats, Andreas Mavrandonakis, Jian Liu, Zhihengyu Chen, Zhijie Chen, Zhanyong Li, Andrey A. Yakovenko, Leighanne C. Gallington, Joseph T. Hupp, Omar K. Farha, Christopher J. Cramer, and Karena W. Chapman*

Read Online

ACCESS | 📊 Metrics & More | 📰 Article Recommendations | 🔲 Supporting Information

ABSTRACT: How molecules approach, bind at, and release from catalytic sites is key to heterogeneous catalysis, including for emerging metal−organic framework (MOF)-based catalysts. We use *in situ* synchrotron X-ray scattering analysis to evaluate the dominant binding sites for reagent and product molecules in the vicinity of catalytic Ni-oxo clusters in NU-1000 with different surface functionalization under conditions approaching those used in catalysis. The locations of the reagent and product molecules within the pores can be linked to the activity for ethylene hydrogenation. For the most active catalyst, ethylene reagent molecules bind close to the catalytic clusters, but only at temperatures approaching experimentally observed onset of catalysis. The ethane product molecules favor a different binding location suggesting that the product is readily released from the active site. An unusual guest-dependence of the framework negative thermal expansion is documented. We hypothesize that reagent and product binding sites reflect the pathway through the MOF to the active site and can be used to identify key factors that impact the catalytic activity.

Heterogeneous catalysts are complex chemical ecosystems. Their catalytic activity and selectivity are a function of cooperative interactions between the active site, the molecular reagents and product, and the surrounding environment which controls access to the active site.[1−4] The importance of the environment surrounding the active site is well recognized for nature's catalysts, enzymes. For inorganic catalysts, the catalyst support and local environment can play a similarly important role,[5,6] although these effects are difficult to explore due, in part, to the challenge in controllably tuning and directly probing the molecular environment around conventional heterogeneous catalysts, for example, supported on metal-oxide nanoparticles. Beyond stabilizing the structure of the catalytic species, the support can control access to the active site, can perturb the atomic and electronic structure of the active site, and can activate the reacting molecules. Elucidating these complex cooperative interactions in inorganic catalysts is important to understanding and tailoring their catalytic activity and selectivity.

The development of crystalline metal−organic frameworks (MOFs) incorporating active catalytic sites[7−11] affords new opportunity to explore the interplay between the catalytic function and the environment mediates access of reagent and product species to the active site.[12−14] Synthetic strategies have been established to precisely functionalize the internal surfaces of a MOF[15−19] and tune the environment surrounding the active site. Crystallographic tools can locate molecular binding sites within the MOF pores, as has been demonstrated in the context of low temperature gas storage applications,[20−22] with emerging approaches such as differential envelope density (DED) analysis allowing dynamically disordered sites to be resolved, even at elevated reaction temperatures.[23]

Here we locate reagent and product species within MOF-catalysts based on NU-1000 (Figure 1) using DED analysis of synchrotron-based *in situ* powder X-ray diffraction, and thereby gain insight into the role of the pore environment in controlling access to the active site. We focus on catalytic
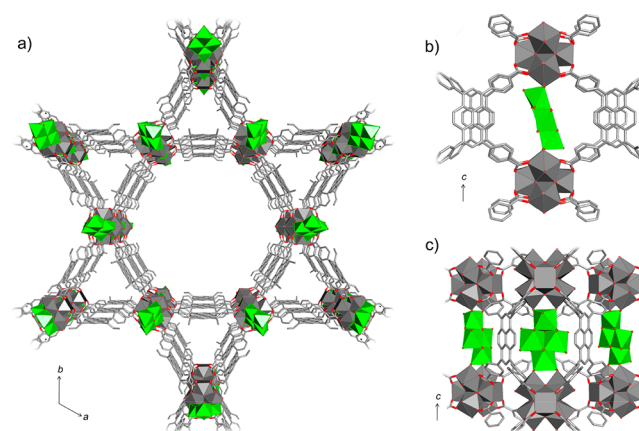

Figure 1. Representations of Ni-NU1000 viewed (a) down the hexagonal and triangular channels and showing the catalytic Ni-oxo clusters (green) viewed from (b) the hexagonal and (c) triangular channels.

Ni-oxo clusters ($Ni_4O_xH_y$) supported on NU-1000 (Ni-NU1000) which catalyze the dimerization and hydrogenation of light alkenes.[9,19,24] Ligand substitution at the Zr_6-based node modifies the activity and selectivity of these reactions.[19] We hypothesize that changes in node chemistry impact how the reagent can approach the active site, thereby contributing to the observed differences in catalytic performance.

The NU-1000 framework defines hexagonal and triangular channels through which molecules access the catalytic Ni-oxo clusters (Figure 1).[25] The catalytic Ni-oxo clusters are located in small pores which connect these channels, and link the Zr_6-based nodes along the c axis.[24] The Ni_4 plane of the Ni-oxo cluster is oriented toward the triangular channel. The native hydroxo-substituted Ni-NU1000 has a turnover frequency for ethylene to ethane conversion that is 2 orders of magnitude higher than fluoroacetylacetonate (Facac) functionalized Ni-NU1000 (Ni-Facac) (see Supporting Information).

In situ X-ray scattering data ($\lambda = 0.2114$ Å) were collected at beamline 11-ID-B at the Advanced Photon Source, at Argonne National Laboratory for Ni-NU1000, Ni-Facac, and Ni-free NU-1000. Following activation at 200 °C in 3.5% H_2 in He, data were collected under ethylene, ethane, and 3.5% H_2 in He gas flow at 10 °C intervals from 40 and 100 °C. Changes in the peak intensities observed for different gases and at different temperatures reflect differences in the distribution of adsorbed guest molecules. The electron density associated with the adsorbed guests was visualized as the DED,[21,26] obtained by subtracting the structure envelope[27,28] for the guest-free system measured under 3.5% H_2 in He at an intermediate temperature (70 °C).[26]

Electron density associated with ethylene and ethane guests is localized within the triangular channels, distributed over three sites depending on the NU-1000 functionalization, temperature, and molecular species (Figure 2). No significant
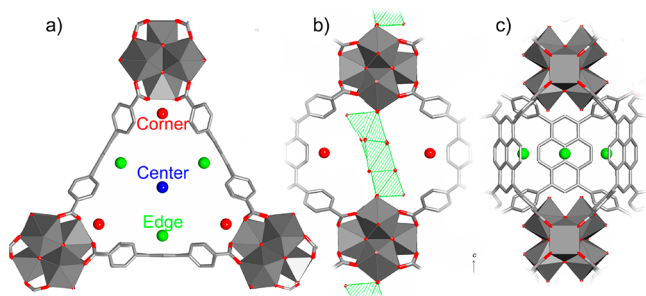

Figure 2. Three principal adsorption sites observed for ethylene and ethane in the present NU-1000 systems, at the center, edge, and corner of the triangular channels. The closest ethylene reagent site is centered over the face of the Ni_4 cluster (green polyhedra).

guest density is observed in the hexagonal channels. The guest sites are centered on the same $z = ^1/_2$ plane as the Ni-oxo cluster and pyrene groups of the ligand. The guest-binding sites are located at the center of the channel at ($^1/_3$, $^2/_3$, $z\sim^1/_2$), the edge of the channel close to the pyrene moiety ($^1/_4$, $^3/_4$, $^1/_2$), and the corner of the channel in proximity to the Ni-oxo clusters ($^1/_2-x$, $^1/_2+x$, $^1/_2$).

We associate the electron density at these sites with different guest−framework interactions:

- At the center of the channel, guests are either delocalized, without strong interactions with the framework surface, or condensed in the pore, with strong interactions with other guest molecules.
- At the edges, guests can interact with the pyrene ligand via π−π or CH−π interactions.
- At the corners closest to the Ni-oxo catalyst, guests can interact with the Ni-oxo catalyst or the phenyl rings.

For the most catalytically active system, Ni-NU1000, the most populated guest-binding site depends strongly on the guest species and temperature (Figure 3). The site favored by ethylene evolves from the corner (i.e., close to the clusters) to the edge (i.e., near the pyrene) to the center sites upon cooling from reaction temperature (100 °C). The ethane reagent does not favor the corner sites but remains at channel edge sites or delocalized in the center of the channel.

For catalyst-free NU-1000, similar distributions were observed for ethane and ethylene (Figure 3). The guests are localized at the corner sites at high temperature, with extra density at the center-site upon cooling, owing to condensation in the channel at higher loadings.

For the poorly active Ni-Facac, where the Facac appears to bind to the Zr_6-based node in the hexagonal channels, the ethylene and ethane molecules are predominately delocalized in the center of the triangular channel with some density at the channel edges (Figure 3).

Periodic density functional theory (DFT) calculations show a correspondence of ethylene and ethane binding site energetics in NU-1000 (Table 1) with the experimentally observed binding sites, validating this approach. Details of the computational approach are given in the SI. As seen experimentally, the energetically favored site for a single ethane or ethylene molecule, which is occupied at the lowest loading (i.e., highest temperature), is at the corner of the triangular channels. The center of the channel is least favored for a single guest molecule but becomes stabilized with loading of multiple guests due to the additional interactions between adsorbed molecules. To probe the importance of the lateral interactions between adsorbed species, a high loading conformation was calculated, with three ethylene molecules at the corners of the triangular pore and a fourth at the center. While the binding energy of the fourth molecule with the NU-1000 framework is only −4.4 kJ·mol^{-1}, its interaction with the other three ethylene molecules amounts to −8.7 kJ·mol^{-1}. Thus, the lateral interactions between the adsorbed molecules become important at high loadings. This is consistent with the increased density observed in the center of the pore at the highest loading (i.e., lowest temperature). Due to the disordered distortions for catalytic Ni-NU1000,[24] its guest-binding energetics could not be straightforwardly modeled.

The molecular binding sites observed for Ni-NU1000 supports its high activity for catalytic ethylene to ethane conversion. For catalysis to occur, ethylene molecules must adsorb and travel through the framework channels, or across the surface to reach the active site. The resultant ethane molecules must release easily. At the highest temperature, the favored ethylene site is closest to the Ni catalyst. The fact that this site only becomes dominant at temperatures approaching the onset of catalysis, with its proximity to the catalytic Ni-oxo cluster, suggests that adsorption here is an important step in the catalysis. The preference of ethane for sites that are more remote from the catalytic cluster also favors efficient catalysis; once ethylene reacts to form ethane, it is readily removed from near the active site. Similarly, the absence of significant
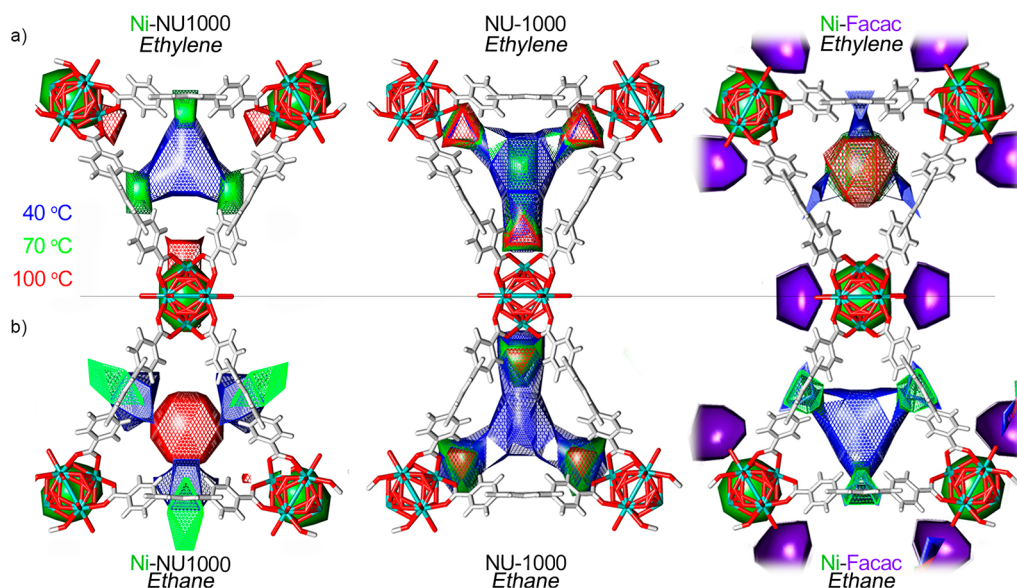
Figure 3. DEDs (mesh) corresponding to the locations of (a) ethylene reagent and (b) ethane product within NU-1000 at 40, 70, and 100 °C (viewed perpendicular to the *c* axis). The principal electron density of the Ni-oxo clusters (between Zr_6 nodes) in Ni-Facac and Ni-NU1000 are shown in solid green. The principal Facac electron density in Ni-Facac is shown in purple.

Table 1. DFT (PBE-D3) Binding Energies Per Molecule in NU-1000

	Ethane	Ethylene
	ΔE ($\Delta\Delta E$)[a]/ kJ·mol^{-1}	ΔE ($\Delta\Delta E$)[a]/kJ·mol^{-1}
Corner	−21.1 (0)	−25.2 (0)
Edge	−19.2 (+1.9)	−16.9 (+8.3)
Small Pore	−13.2 (+7.9)	−13.6 (+11.6)
Center	−8.0 (+13.1)	−5.8 (+19.4)

[a]Values in parentheses are energy differences with respect to the strongest binding site.

ethylene density close to the active site in Ni-Facac can be linked to the substantially lower catalytic activity for the system. The difference in preferred ethylene binding, compared to Ni-NU1000, may be of steric or electronic origin.

While we see progressive filling and overlap of different adsorption sites at different temperatures for NU-1000 and Ni-Facac, based on our understanding of guest adsorption in MOFs, it is unusual that the principal adsorption site would change with temperature as seen for ethylene in Ni-NU1000. Based on enthalpic considerations, the lowest energy (strongest) binding sites would be expected to fill first, with progressive filling of weaker binding sites as the guest occupancy is increased, in this case, with cooling. For ethylene in Ni-NU1000, the most energetically favorable binding site appears to be temperature dependent, an observation that is consistent with an unusual guest-dependence of the anomalous thermal expansion behavior seen for Ni-NU1000, but not NU-1000 or Ni-Facac. Interestingly, the lattice thermal expansion varies significantly with the guest for catalytically active Ni-NU1000, but not for Ni-Facac. Anisotropic thermal expansion in an ethylene atmosphere (α_a = +11 × 10^{-6} K^{-1}; α_c = −65 × 10^{-6} K^{-1}), but near zero thermal expansion in ethane or dilute hydrogen (see Supporting Information), was determined for Ni-NU1000. Negative thermal expansion in framework solids is associated with low energy lattice vibrations.[29−31] While sorption and steric interactions with guest species can dampen these lattice vibrations and, accordingly, the magnitude of

thermal expansion,[32,33] it is unusual that this does not similarly affect all NU-1000 phases.[34] This observation may be explained by the markedly different guest binding location for ethylene or electronic interaction for the ethylene molecule that impacts the lattice vibrations.

In summary, the approach demonstrated here represents a new strategy to explore how molecules approach a catalytic site and how this impacts catalytic performance. We gain insight into the relative energetics of gas-binding under conditions relevant to catalysis. The locations found for the reagent and product molecules can suggest a basis for performance differences in differently functionalized systems. These include the proximity of the reagent to the catalytic site or competitive binding of the product at the active site, insights valuable to designing high performance catalysts. While the present study suggests that adsorption over the plane of edge-sharing Ni-oxo octahedra is a key step in the catalytic process, given the correspondence of the occupation of this site with the onset of catalysis, ethylene adsorption at this site is clearly an important step in the catalysis mechanism. This may represent a pathway to the active site or the active site itself; it serves as an experimental starting configuration for computational studies of potential reaction mechanisms. The observation of this overplane site is particularly interesting since the edges have been proposed to be important in other layered architectures, albeit for more extended layers.[35] Extensions of this approach can be envisioned to simulated reaction conditions and to understand other porous crystalline catalysis, including other MOFs and zeolites.

■ ASSOCIATED CONTENT

Ⓢ Supporting Information

The Supporting Information is available free of charge at https://pubs.acs.org/doi/10.1021/jacs.1c11213.

Details of the material synthesis, catalysis, X-ray scattering analysis, and computation (PDF)

■ AUTHOR INFORMATION

Corresponding Author

Karena W. Chapman − *X-ray Science Division, Advanced Photon Source, Argonne National Laboratory, Argonne, Illinois 60439, United States; Department of Chemistry, Stony Brook University, Stony Brook, New York 11790, United States;* ⓞ orcid.org/0000-0002-8725-5633; Email: karena.chapman@stonybrook.edu

Authors

Ana E. Platero-Prats − *X-ray Science Division, Advanced Photon Source, Argonne National Laboratory, Argonne, Illinois 60439, United States;* Present Address: Universidad Autónoma de Madrid, Madrid, 28049, Spain; ⓞ orcid.org/0000-0002-2248-2739

Andreas Mavrandonakis − *Department of Chemistry, Chemical Theory Center, and Supercomputing Institute, University of Minnesota, Minneapolis, Minnesota 55455, United States;* Present Address: Electrochemical Processes Unit, IMDEA Energy, Móstoles, 28935, Spain; ⓞ orcid.org/0000-0002-5053-8154

Jian Liu − *Department of Chemistry, Northwestern University, Evanston, Illinois 60208, United States;* ⓞ orcid.org/0000-0002-5024-1879

Zhihengyu Chen − *Department of Chemistry, Stony Brook University, Stony Brook, New York 11790, United States*

Zhijie Chen − *Department of Chemistry, Northwestern University, Evanston, Illinois 60208, United States;* ⓞ orcid.org/0000-0001-9232-7382

Zhanyong Li − *Department of Chemistry, Northwestern University, Evanston, Illinois 60208, United States*

Andrey A. Yakovenko − *X-ray Science Division, Advanced Photon Source, Argonne National Laboratory, Argonne, Illinois 60439, United States*

Leighanne C. Gallington − *X-ray Science Division, Advanced Photon Source, Argonne National Laboratory, Argonne, Illinois 60439, United States;* ⓞ orcid.org/0000-0002-0383-7522

Joseph T. Hupp − *Department of Chemistry, Northwestern University, Evanston, Illinois 60208, United States;* ⓞ orcid.org/0000-0003-3982-9812

Omar K. Farha − *Department of Chemistry and Department of Chemical and Biological Engineering, Northwestern University, Evanston, Illinois 60208, United States;* ⓞ orcid.org/0000-0002-9904-9845

Christopher J. Cramer − *Department of Chemistry, Chemical Theory Center, and Supercomputing Institute, University of Minnesota, Minneapolis, Minnesota 55455, United States;* Present Address: Underwriters Laboratories Inc., Northbrook, Illinois, 60062, United States; ⓞ orcid.org/0000-0001-5048-1859

Complete contact information is available at:
https://pubs.acs.org/10.1021/jacs.1c11213

Notes

The authors declare no competing financial interest.

■ REFERENCES

(1) Koval, C. A.; Lercher, J.; Scott, S. L. *Report of the Basic Research Needs Workshop for Catalysis Science*; Department of Energy: 2018.

(2) Li, H.; Xiao, J.; Fu, Q.; Bao, X. Confined catalysis under two-dimensional materials. *Proc. Natl. Acad. Sci. U. S. A.* **2017**, *114* (23), 5930−5934.

(3) Burgess, S. A.; Appel, A. M.; Linehan, J. C.; Wiedner, E. S. Changing the Mechanism for CO2 Hydrogenation Using Solvent-Dependent Thermodynamics. *Angew. Chem., Int. Ed.* **2017**, *56* (47), 15002−15005.

(4) Feng, X.; Song, Y.; Chen, J. S.; Xu, Z.; Dunn, S. J.; Lin, W. Rational Construction of an Artificial Binuclear Copper Monooxygenase in a Metal−Organic Framework. *J. Am. Chem. Soc.* **2021**, *143* (2), 1107−1118.

(5) Chen, Y.; Ma, S. Biomimetic catalysis of metal−organic frameworks. *J. Chem. Soc., Dalton Trans.* **2016**, *45* (24), 9744−9753.

(6) Syed, Z. H.; Sha, F.; Zhang, X.; Kaphan, D. M.; Delferro, M.; Farha, O. K. Metal−Organic Framework Nodes as a Supporting Platform for Tailoring the Activity of Metal Catalysts. *ACS Catal.* **2020**, *10* (19), 11556−11566.

(7) Yang, D.; Gates, B. C. Catalysis by Metal Organic Frameworks: Perspective and Suggestions for Future Research. *ACS Catal.* **2019**, *9* (3), 1779−1798.

(8) Bavykina, A.; Kolobov, N.; Khan, I. S.; Bau, J. A.; Ramirez, A.; Gascon, J. Metal−Organic Frameworks in Heterogeneous Catalysis: Recent Progress, New Trends, and Future Perspectives. *Chem. Rev.* **2020**, *120* (16), 8468−8535.

(9) Li, Z.; Schweitzer, N. M.; League, A. B.; Bernales, V.; Peters, A. W.; Getsoian, A.; Wang, T. C.; Miller, J. T.; Vjunov, A.; Fulton, J. L.; Lercher, J. A.; Cramer, C. J.; Gagliardi, L.; Hupp, J. T.; Farha, O. K. Sintering-Resistant Single-Site Nickel Catalyst Supported by Metal Organic Framework. *J. Am. Chem. Soc.* **2016**, *138* (6), 1977−1982.

(10) Yuan, S.; Zou, L. F.; Li, H. X.; Chen, Y. P.; Qin, J. S.; Zhang, Q.; Lu, W. G.; Hall, M. B.; Zhou, H. C. Flexible Zirconium Metal-Organic Frameworks as Bioinspired Switchable Catalysts. *Angew. Chem., Int. Ed.* **2016**, *55* (36), 10776−10780.

(11) Zhang, T.; Manna, K.; Lin, W. B. Metal-Organic Frameworks Stabilize Solution-Inaccessible Cobalt Catalysts for Highly Efficient Broad-Scope Organic Transformations. *J. Am. Chem. Soc.* **2016**, *138* (9), 3241−3249.

(12) Liu, L.; Zhou, T.-Y.; Telfer, S. G. Modulating the Performance of an Asymmetric Organocatalyst by Tuning Its Spatial Environment in a Metal−Organic Framework. *J. Am. Chem. Soc.* **2017**, *139* (39), 13936−13943.

(13) Li, Y.-M.; Yuan, J.; Ren, H.; Ji, C.-Y.; Tao, Y.; Wu, Y.; Chou, L.-Y.; Zhang, Y.-B.; Cheng, L. Fine-Tuning the Micro-Environment to Optimize the Catalytic Activity of Enzymes Immobilized in Multivariate Metal−Organic Frameworks. *J. Am. Chem. Soc.* **2021**, *143* (37), 15378−15390.

(14) Johnson, B. A.; Beiler, A. M.; McCarthy, B. D.; Ott, S. Transport Phenomena: Challenges and Opportunities for Molecular Catalysis in Metal−Organic Frameworks. *J. Am. Chem. Soc.* **2020**, *142* (28), 11941−11956.

(15) Cohen, S. M. The Postsynthetic Renaissance in Porous Solids. *J. Am. Chem. Soc.* **2017**, *139* (8), 2855−2863.

(16) Islamoglu, T.; Goswami, S.; Li, Z.; Howarth, A. J.; Farha, O. K.; Hupp, J. T. Postsynthetic Tuning of Metal−Organic Frameworks for Targeted Applications. *Acc. Chem. Res.* **2017**, *50* (4), 805−813.

(17) Kim, M.; Cahill, J. F.; Fei, H.; Prather, K. A.; Cohen, S. M. Postsynthetic Ligand and Cation Exchange in Robust Metal−Organic Frameworks. *J. Am. Chem. Soc.* **2012**, *134* (43), 18082−18088.

(18) Takaishi, S.; DeMarco, E. J.; Pellin, M. J.; Farha, O. K.; Hupp, J. T. Solvent-assisted linker exchange (SALE) and post-assembly metallation in porphyrinic metal-organic framework materials. *Chem. Sci.* **2013**, *4* (4), 1509−1513.

(19) Liu, J.; Ye, J.; Li, Z.; Otake, K.-i.; Liao, Y.; Peters, A. W.; Noh, H.; Truhlar, D. G.; Gagliardi, L.; Cramer, C. J.; Farha, O. K.; Hupp, J. T. Beyond the Active Site: Tuning the Activity and Selectivity of a Metal−Organic Framework-Supported Ni Catalyst for Ethylene Dimerization. *J. Am. Chem. Soc.* **2018**, *140* (36), 11174−11178.

(20) Rowsell, J. L. C.; Spencer, E. C.; Eckert, J.; Howard, J. A. K.; Yaghi, O. M. Gas adsorption sites in a large-pore metal-organic framework. *Science* **2005**, *309* (5739), 1350−1354.

(21) Chen, Y.-P.; Liu, Y.; Liu, D.; Bosch, M.; Zhou, H.-C. Direct Measurement of Adsorbed Gas Redistribution in Metal−Organic Frameworks. *J. Am. Chem. Soc.* **2015**, *137* (8), 2919−2930.

(22) McDonald, T. M.; Mason, J. A.; Kong, X.; Bloch, E. D.; Gygi, D.; Dani, A.; Crocellà, V.; Giordanino, F.; Odoh, S. O.; Drisdell, W. S.; Vlaisavljevich, B.; Dzubak, A. L.; Poloni, R.; Schnell, S. K.; Planas, N.; Lee, K.; Pascal, T.; Wan, L. F.; Prendergast, D.; Neaton, J. B.; Smit, B.; Kortright, J. B.; Gagliardi, L.; Bordiga, S.; Reimer, J. A.; Long, J. R. Cooperative insertion of CO2 in diamine-appended metal-organic frameworks. *Nature* **2015**, *519*, 303.

(23) Gallington, L. C.; Kim, I. S.; Liu, W. G.; Yakovenko, A. A.; Platero-Prats, A. E.; Li, Z. Y.; Wang, T. C.; Hupp, J. T.; Farha, O. K.; Truhlar, D. G.; Martinson, A. B. F.; Chapman, K. W. Regioselective Atomic Layer Deposition in Metal-Organic Frameworks Directed by Dispersion Interactions. *J. Am. Chem. Soc.* **2016**, *138* (41), 13513−13516.

(24) Platero-Prats, A. E.; League, A. B.; Bernales, V.; Ye, J. Y.; Gallington, L. C.; Vjunov, A.; Schweitzer, N. M.; Li, Z. Y.; Zheng, J.; Mehdi, B. L.; Stevens, A. J.; Dohnalkova, A.; Balasubramanian, M.; Farha, O. K.; Hupp, J. T.; Browning, N. D.; Fulton, J. L.; Camaioni, D. M.; Lercher, J. A.; Truhlar, D. G.; Gagliardi, L.; Cramer, C. J.; Chapman, K. W. Bridging Zirconia Nodes within a Metal-Organic Framework via Catalytic Ni-Hydroxo Clusters to Form Hetero-bimetallic Nanowires. *J. Am. Chem. Soc.* **2017**, *139* (30), 10410−10418.

(25) Mondloch, J. E.; Bury, W.; Fairen-Jimenez, D.; Kwon, S.; DeMarco, E. J.; Weston, M. H.; Sarjeant, A. A.; Nguyen, S. T.; Stair, P. C.; Snurr, R. Q.; Farha, O. K.; Hupp, J. T. Vapor-Phase Metalation by Atomic Layer Deposition in a Metal−Organic Framework. *J. Am. Chem. Soc.* **2013**, *135* (28), 10294−10297.

(26) Yakovenko, A. A.; Wei, Z.; Wriedt, M.; Li, J.-R.; Halder, G. J.; Zhou, H.-C. Study of Guest Molecules in Metal−Organic Frameworks by Powder X-ray Diffraction: Analysis of Difference Envelope Density. *Cryst. Growth Des.* **2014**, *14* (11), 5397−5407.

(27) McCusker, L. B.; Baerlocher, C. Using electron microscopy to complement X-ray powder diffraction data to solve complex crystal structures. *Chem. Commun.* **2009**, No. 12, 1439−1451.

(28) Yakovenko, A. A.; Reibenspies, J. H.; Bhuvanesh, N.; Zhou, H.-C. Generation and applications of structure envelopes for porous metal-organic frameworks. *J. Appl. Crystallogr.* **2013**, *46* (2), 346−353.

(29) Wu, Y.; Kobayashi, A.; Halder, G. J.; Peterson, V. K.; Chapman, K. W.; Lock, N.; Southon, P. D.; Kepert, C. J. Negative Thermal Expansion in the Metal-Organic Framework Material Cu$_3$(1,3,5-benzenetricarboxylate)$_2$. *Angew. Chem., Int. Ed.* **2008**, *47*, 8929−8932.

(30) Dubbeldam, D.; Walton, K. S.; Ellis, D. E.; Snurr, R. Q. Exceptional Negative Thermal Expansion in Isoreticular Metal-Organic Frameworks. *Angew. Chem., Int. Ed.* **2007**, *46* (24), 4496−4499.

(31) Cliffe, M. J.; Hill, J. A.; Murray, C. A.; Coudert, F.-X.; Goodwin, A. L. Defect-dependent colossal negative thermal expansion in UiO-66(Hf) metal-organic framework. *Phys. Chem. Chem. Phys.* **2015**, *17* (17), 11586−11592.

(32) Goodwin, A. L.; Chapman, K. W.; Kepert, C. J. Guest-dependent negative thermal expansion in nanoporous Prussian Blue analogues (MPtIV)-Pt-II(CN)(6)center dot x{H2O} ($0 \leq x \leq 2$; M = Zn, Cd). *J. Am. Chem. Soc.* **2005**, *127* (51), 17980−17981.

(33) Gao, Q.; Chen, J.; Sun, Q.; Chang, D.; Huang, Q.; Wu, H.; Sanson, A.; Milazzo, R.; Zhu, H.; Li, Q.; Liu, Z.; Deng, J.; Xing, X. Switching Between Giant Positive and Negative Thermal Expansions of a YFe(CN)6-based Prussian Blue Analogue Induced by Guest Species. *Angew. Chem., Int. Ed.* **2017**, *56* (31), 9023−9028.

(34) Lu, Z.; Liu, J.; Zhang, X.; Liao, Y.; Wang, R.; Zhang, K.; Lyu, J.; Farha, O. K.; Hupp, J. T. Node-Accessible Zirconium MOFs. *J. Am. Chem. Soc.* **2020**, *142* (50), 21110−21121.

(35) Du, P.; Kokhan, O.; Chapman, K. W.; Chupas, P. J.; Tiede, D. M. Elucidating the Domain Structure of the Cobalt Oxide Water Splitting Catalyst by X-ray Pair Distribution Function Analysis. *J. Am. Chem. Soc.* **2012**, *134* (27), 11096−11099.